Foil activation studies of spectral variations in the MUSE4 critical configuration

M. Plaschy, R. Chawla, C. Destouches, C. Domergue, H. Servière, P. Chaussonnet, J. M. Laurens, R. Soule, G. Rimpault

PHYSOR 2002, Seoul, Korea, October 7-10, 2002

FOIL ACTIVATION STUDIES OF SPECTRAL VARIATIONS IN THE MUSE4 CRITICAL CONFIGURATION

M. Plaschy, R. Chawla

Swiss Federal Institute of Technology (EPFL) and Paul Scherrer Institute (PSI)
Laboratory for Reactor Physics and Systems Behaviour (LRS)
1015 Lausanne, SWITZERLAND
E-mail : michael.plaschy@epfl.ch

C. Destouches, C. Domergue, H. Servière, P. Chaussonnet,
J.M. Laurens, R. Soule, G. Rimpault

Commissariat à l'Energie Atomique (CEA), Centre d'Etudes de Cadarache
Département d'Etudes des Réacteurs (DER)
13108 Saint Paul lez Durance Cedex, FRANCE
E-mail : christophe.destouches@cea.fr

ABSTRACT

The MUSE4 phase of the MUSE (Multiplication with an external source) programme has been launched recently at the MASURCA facility at Cadarache (France). This series of integral experiments relevant to accelerator driven systems (ADSs) consists in studying a reference critical fast-spectrum configuration, followed by three different subcritical modifications of the same, each driven by an external neutron source produced via an accelerator. The presence of the accelerator tube in the core creates new types of heterogeneities, the effects of which need to be modelled and quantified by appropriate calculational tools. A part of the unique ADS-relevant validation base being provided by MUSE4 are results from a wide range of activation foil measurements covering various reaction rates, both with and without thresholds. Each experimental campaign consists in irradiating the foils in different representative locations to characterise the new types of spectral variations. This paper presents experimental results obtained in the reference critical MUSE4 configuration. Comparisons are made with calculations using both deterministic (ERANOS-1.2) and stochastic (MCNP-4C) codes in conjunction with different data libraries (JEF-2.2, ERALIB1, ENDF/B6). Good agreement has been obtained between calculation and experiment in most cases. However, significant discrepancies have been found for the high-threshold reaction rates inside and around the central diffusing lead region, indicating the need for more detailed investigations in this context.

1. INTRODUCTION

Waste management considerations have led to the study of the transmutation capabilities of accelerator driven systems (ADSs) as an alternative to conventional reactors, since these avoid safety problems related to the very low β_{eff} values of the minor actinides such as Np and Am. In this context, it is necessary to extend the validation domain of calculational methods and data developed for critical fast reactors to the analysis of such source-driven subcritical systems. For example, the presence of an accelerator tube and a diffusing medium at the centre of the core creates unusual types of spectral variations which need to be predicted correctly. Effectively, accurate knowledge of the energy and spatial dependence of the neutron flux is essential for assessing characteristics such as the impact of the external source on power peaking and irradiation damage effects.

It is in the above context that an extensive experimental programme, MUSE4, has been established at the MASURCA facility at CEA-Cadarache (France) [1]. This programme consists of studies in a reference critical fast-spectrum configuration, followed by three different, source-driven subcritical modifications of the same. Two major aspects will be analysed during the MUSE4 project. Firstly, different dynamics measurements, e.g. to obtain the subcriticality level, will be developed, tested and compared. Secondly, specific static measurements will be performed for characterisation of the neutronic spectrum variations (a) by using a set of miniature fission chambers (U^{235}, U^{238}, Np^{237}, Pu^{239}, Pu^{240}, Am^{241},…) and (b) by irradiating various types of activation foils (indium, iron, cobalt, nickel, zinc,…) in the regions of interest, principally near the accelerator/lead, lead/fuel and fuel/reflector interfaces, where the new types of spectral fluctuations are the more important.

The current paper presents the results of foil activation measurements performed in the reference critical configuration. Comparisons are made with calculations using ERANOS-1.2 [2] and MCNP-4C [3] (in conjunction with different nuclear data libraries) to interpret the experimental results and to investigate the capabilities of the applied codes to reproduce the spectral variations in terms of reaction rate variations across the new types of heterogeneities. At a later stage, the currently reported experimental results will also be used, employing a suitable unfolding code, to yield the neutron spectra at certain characteristic locations in the assembly.

2. DESCRIPTION OF THE MUSE4 CONFIGURATIONS

In the MUSE4 experiments, the whole-reactor configuration essentially consists of five different regions, set up as an arrangement of tubes of 10.6 x 10.6 x 230.44 cm^3, each presenting a different axial-zone structure. It is convenient to describe the individual MUSE4 regions starting from the inside of the assembly.

The presence of the accelerator tube at the centre creates a specific region which crosses the reactor completely along the mid-plane until reaching the outside. In front of the accelerator

tube, which has a lead/aluminium clad, there is a lead diffusing region which serves mainly to obtain a certain symmetry of the power distribution. These two regions, with their associated heterogeneity effects, represent ADS-specific particularities. The fuel zone consists of about 70 assemblies of PuO2/UO2+Na and is hence characteristic of a standard fast reactor core. Slightly different Pu^{239} enrichments are employed for the fuel above and below the accelerator tube. The MOX zone is surrounded by a reflector region, constituted by sodium and stainless steel rods. Finally the external zone of the reactor consists of stainless steel shielding. A horizontal cross-sectional view of the MUSE4 critical configuration is given in Figure 1.

Even though this paper only reports on measurements in the reference critical configuration, it is important to mention that the three different source-driven subcriticals to follow will have k_{eff} values between 0.950 and 0.995. These configurations will be very similar in layout to the critical loading, except that a small number of fuel assemblies will be replaced by reflector assemblies to obtain the desired degree of subcriticality. In each subcritical configuration, the deuteron accelerator (GENEPI) will be used in the two different modes possible, viz. to produce neutrons of either 2.7 MeV via the $D(d,n)He^3$ reaction or of 14 MeV via the $T(d,n)He^4$ reaction. The corresponding measurements will thus enable a useful generic assessment of the impact of an external source.

To introduce activation foils in different locations of the MASURCA facility, experimental channels have been provided. These channels have a section of 1.27cm x 1.27cm, which limits the size of the activation foils which can be used. A description of the experimental setup is presented in the following section.

3. EXPERIMENTAL PROCEDURES

The foil activation measurements carried out in the reference critical configuration are described in this section, a discussion being included on the achievable levels of accuracy for the different locations

3.1 ACTIVATION FOILS AND EXPERIMENTAL SETUP

The choice of foils has been guided mainly by the need to cover as wide a range of threshold energy values as possible. The full list of activation reactions employed is given in Table 1 (particular care was taken to ensure high-purity foil material). Most of the foils are disc-shaped with a thickness of 0.25mm and a diameter of 9mm. However, each of the NpO_2 samples used consists of 9 spheres of 0.8mm diameter contained in a titanium box. All activation samples were located inside experimental aluminium rods, which have a section of 10mm x 10mm. These rods were inserted into two radial channels (along the west/east and north/south axes, respectively) and one axial channel (in the lead region), as indicated in Figure 1. On the basis of calculations using MCNP-4C and ERANOS-1.2 codes, 10 different

locations were selected for the reference MUSE4 configuration (critical, without source) for activation foil irradiations. These locations are indicated by 1-6 and A-D in Figure 1. Location 1 has been considered as a reference point in an unperturbed region near a calibrated fission chamber. Location 2 permits study of the impact of the lead region, while positions 3 and 4 have been selected for highlighting the potential core asymmetry. Location 5 characterises lead moderation/multiplication effects, while location 6 provides a useful test of code capabilities to treat streaming effects along the voided accelerator-tube region. Finally, locations A, B, C and D permit study of spectral variations along the west-east axis.

3.2 CORRECTIONS APPLIED AND MEASUREMENT ACCURACIES

The achievement of accurate foil activation measurements requires particular attention being given to the application of necessary corrections and the treatment of experimental uncertainties. (The γ-spectrometry measurements are performed in a Cadarache laboratory accredited by COFRAC, the French Accreditation Committee.) The corrections to be applied result from either the irradiation conditions or from physical effects associated with the γ-counting of the irradiated foils:

• Corrections due to the irradiation conditions

Each type of foil needs to be activated differently depending on the half-life of the activation product and the reaction cross section. Consequently, it has been necessary to perform 4 different irradiations to activate the complete set of samples. In more specific terms, the first irradiation lasted 1.5h at ~150W, the second 6h at ~1500W, the third 3.5h at ~1500W and the last one 2h at ~200W. A calibration factor, obtained with the aid of different monitors distributed within the reactor, was determined to normalise the individual irradiations among each other, and this could be done to within an uncertainty (1-sigma) of 2%. Obviously, the calibration factor needs to be applied to the saturated activities, which are obtained from the following relation:

$$A_{sat}=\frac{A}{1-\exp(-t\lambda)} \tag{1}$$

where A_{sat} is the saturated activity, A is the measured activity, t is the irradiation time and λ is the disintegration constant of the considered isotope. For completeness, it may be mentioned that the saturated activity is directly related to the measured reaction rate via:

$$A_{sat}=m_o \int_{E_S}^{\infty} \sigma_{mn}(E)\varphi(E)dE \tag{2}$$

where m_o is the number of target nuclei in the sample, $\sigma_{mn}(E)$ is the reaction cross section which produces nuclei of type n, $\varphi(E)$ is the neutron flux and E_s is the threshold energy for the reaction.

Self-shielding effects for the different activation foils (which effectively reduce the measured reaction rate, relative to that for an infinitely thin sample) have been estimated numerically with the aid of MCNP-4C simulations. As expected, the corrections are non-negligible only in the case of non-threshold reactions at locations near zones with softer neutron spectra. Certain experimental investigations in this context are presented in the following subsection.

• Corrections concerning the γ-counting of the irradiated foils

There is the need to correct for several different physical effects during the γ-counting. Firstly, depending on the disintegration scheme of the activation product and the detector/sample distance (but independent of the activity level), some γ-emission coincidences occur, yielding less counts under the considered peak. This effect has been quite important in our case: ~7% for In^{116m} (from In^{115m}), ~5% for Na^{24} (from Al^{27} or Mg^{24}), ~3% for Mn^{56} (from Fe^{56}),…

Secondly, as it is largely threshold reactions which are being considered, the activity of the counted foils is generally low. This necessitates the use of the closest possible distance between the foil and the HPGe γ-detector in order to achieve acceptable statistical accuracies. Nevertheless, it has been possible to obtain, in most of the cases, at least 10000 counts under the considered peak.

Finally, γ-self-absorption effects have been taken into account. This effect is essentially related to γ-energy, and to the thickness and density of the foil material. In general, the corrections applied have been less than 1%. In the case of the lead and thorium foils, however, the corrections were larger, viz. up to 7%.

An accurate determination of the HPGe detector efficiency is important in case absolute activities are needed. This is not essential when considering the ratio, at two different locations, of reaction rates for the same reaction. The γ-spectrometry laboratory uses 12 different reference sources (Am^{241}, Cd^{109}, Ce^{139}, Co^{59}, Mn^{54}, Zn^{65},…) to determine an efficiency curve for each possible distance of a counted sample. An uncertainty of less than 1% (1-sigma) is guaranteed for the calibration factor in each case. However, as the samples being counted rarely have the same geometry as the calibration sources, a correction is needed to take differences into account. In the present case, the corresponding corrections have been almost insignificant due to the relatively small diameter and thickness of the activation foils.

A summary of the achievable experimental accuracies for each studied reaction is presented in Table 1. The indicated uncertainties are quite acceptable for highlighting the principal effects of interest, e.g. the impact of the central lead region, or to verify different experimental aspects such as those described in the following subsection.

3.3 SUBSIDIARY EXPERIMENTAL INVESTIGATIONS

• Reproducibility analysis

To check the reproducibility of the measurements, several different foil types have been used in different irradiations. Considering the assessed uncertainties, excellent agreement was obtained in each case. Thus, for example, for the Ni^{58}(n,p) reaction determined during

irradiations 2 and 3 at all six locations, the average activity ratio between the two irradiations was 0.99 ± 0.02. This is quite a satisfactory result, considering that the two irradiation days were separated by a period of 5 months.

• West/east symmetry verification
The west/east symmetry of the core has been verified experimentally, within the measurement uncertainties, using several different foil types. This confirms the weak impact of the control rod (which is present only on the east side). The verified core symmetry has, in turn, been applied in investigations of foil self-shielding effects, as described below.

• Self-shielding effect measurements
Some specific measurements have been performed to estimate the importance of self-shielding phenomena. Advantage was taken of the west/east symmetry of the core for the purpose. Thus, for a given reaction type, a single foil was placed on the east side of the core and a corresponding 3-foil packet was located at the same distance on the west side. The ratio of the specific activities of the single east-foil and the central foil of the west-side packet clearly provide a measure of self-shielding effect. Values of this ratio are listed for several different foil types and locations in Table 2. The experimental results show that significant self-shielding effects occur only for non-threshold reactions, and that too only near the reflector zone, i.e. at a considerable distance from the core centre (in a less fast spectrum). These measurements confirm the MCNP-4C calculations carried out for estimating foil effects during the experimental planning.

As discussed above, it has generally been possible to achieve adequate experimental accuracies in the current study. Furthermore, the magnitude of the measured spectral variations, as reported in Section 5, amply justify the choice of the foil-location positions which were selected on the basis of preliminary analysis. These are clearly important requirements for qualifying these experiments as providing a valuable set of ADS-relevant integral results.

4. ERANOS-1.2 AND MCNP-4C CALCULATIONS

To interpret the experimental data, comparisons have been made with the two codes ERANOS-1.2 (European Reactor Analysis Optimized System) and MCNP-4C (Monte Carlo N-Particles).
ERANOS-1.2 is a deterministic code consisting of a cell calculation routine (ECCO) and a core calculation module in either 3D (TGV-VARIANT) or in RZ-geometry (BISTRO). Due to the non-cylindrical geometry of the MUSE4 assembly, only the 3D-TGV module has currently been used for the whole-core calculation. The numerical approximations chosen in this context are P1 for the anisotropy treatment of the cross sections and SP3 for the flux (in 33 energy groups). The solution of the transport equation with TGV is carried out in an "even" formulation by a variational method, as given by:

$$-\vec{\Omega}\vec{\nabla}\frac{1}{\Sigma_t(\vec{r})}\vec{\Omega}\vec{\nabla}\psi_+(\vec{r},\vec{\Omega})+\Sigma_t(\vec{r})\psi_+(\vec{r},\vec{\Omega})=\Sigma_s(\vec{r})\phi(\vec{r})+S(\vec{r}) \quad (3)$$

where $\vec{\Omega}$ is the considered solid angle, $\psi_+(\vec{r},\vec{\Omega})$ is the angular even flux, $\Sigma_t(\vec{r})$ is the total macroscopic cross section, $\Sigma_s(\vec{r})$ is the macroscopic scattering cross section, $\phi(\vec{r})$ is the scalar flux and $S(\vec{r})$ is the source term. Due to the $1/\Sigma_t$ term in equation (3), void regions cannot be correctly treated in an explicit manner. It has thus been necessary, in modelling the void region of the accelerator zone, to homogenise it with the associated aluminium/lead clad. ERANOS-1.2 has currently been employed with both the JEF-2.2 [4] nuclear data library and the adjusted ERALIB-1 [5] library.
MCNP-4C is a widely used stochastic code. One of its advantages is the ability to permit an accurate description of the experimental configuration, e.g. in modelling low-density regions such as the accelerator zone. However, the computing time can be very significant with the statistical approach, particularly in obtaining adequate uncertainties for threshold reaction rates. The current MCNP-4C analysis of the experiments has been carried out using the JEF-2.2 library in conjunction with the ENDF/B6 dosimetry data file (see below).
The geometry and material descriptions for creating the numerical ERANOS and MCNP models have been taken from a recent document [6] presenting the specifications for a new international benchmark exercise based on MUSE4.

The currently calculated k_{eff} values for the reference critical MUSE4 configuration are given in Table 3. The ERANOS-1.2 (JEF-2.2) k_{eff} is about 300pcm higher than the MCNP-4C (JEF-2.2) value. This discrepancy is partly explained by the homogenization of the accelerator channel in ERANOS, which underestimates the neutron leakage (assessed to be about 150pcm by a RZ-BISTRO calculation). Good agreement is also obtained between both codes and the experimental k_{eff} result (0.999, after correction for the presence of the pilot rod). Table 3 also clearly indicates the poor prediction of the critical loading with the ENDF/B6 library. Other studies have shown that this is due to the Pu^{239} ν-value (neutrons produced per fission), which is too large.
These k_{eff} comparisons (a) confirm the overall accuracy of the calculational models and (b) show that it is not appropriate to consider the ENDF/B6 library for treating the global neutron transport in MUSE4. The MCNP-4C analysis of the current experiments has accordingly been carried out employing the JEF-2.2 library, although the dosimetry data for computing the threshold reaction rates has been taken from ENDF/B6.

5. COMPARISON OF CALCULATIONAL AND EXPERIMENTAL RESULTS

The results obtained from the current foil activation studies in the critical MUSE4 configuration are presented in this section in three parts. Firstly, calculation/experiment (C/E) values are given for the spatial distribution of different non-threshold reaction rates, i.e. the value of a certain reaction rate at a given location relative to that at a reference position. (Position 1 (P1) has been chosen for the purpose.) This is followed by corresponding C/E

values for threshold reaction rates. Finally, calculated and measured spatial variations of different spectral indices (reaction rate ratios relative to In^{115}(n,n')) are compared at positions P2-P6, relative to the values at P1.

5.1 NON-THRESHOLD REACTION RATES

The three different non-threshold reactions which have been considered here are captures in In^{115}, Co^{59} and Zn^{64}. C/E values for the ratios of saturated activities at P2-P6, relative to P1 in each case, are presented in Table 4 for the different calculational schemes. The results appear very satisfactory when one considers the corresponding uncertainties, except perhaps for P2/P1 with Zn64(n,γ). It is worth noting that the two different libraries JEF-2.2 and ERALIB1 (used by ERANOS) provide very similar results.

5.2 THRESHOLD REACTION RATES

Table 5 gives the corresponding MCNP-based C/E values for the threshold reactions. As mentioned earlier, the ENDF/B6 dosimetry file was used in conjunction with MCNP-4C, although it is the JEF-2.2 library which has been employed for the neutron transport calculation. Although generally satisfactory agreement is obtained for P4-P6, significant discrepancies are indicated for P2 and P3, i.e. the prediction of spectral variations in and around the central lead region at high neutron energies appears to be problematic. Certain further investigations are clearly needed, of both calculational and experimental aspects, to understand these differences.

The spatial variations of two other threshold reactions (Th^{232} and Np^{237} fission) have been studied, this time in terms of traverses along the west/east axis, i.e. with measurements at locations A, B, C and D. Figure 2 shows the comparisons of calculated and experimental results, satisfactory agreement being indicated in the various regions (reflector, fuel, lead) for both ERANOS-1.2 (with JEF-2.2 or ERALIB1) and MCNP-4C (with JEF-2.2). The moderation effects in the central lead region are clearly reflected in the observed decrease of the threshold fission rates.

5.3 SPECTRAL INDICES

In contrast to Tables 4 and 5, which do not provide a direct indication of the neutron spectrum at the different locations, Table 6 presents calculated and experimental spatial variations of several spectral indices. These have been considered in terms of reaction rate ratios, relative to In^{115}(n,n'), at locations P2-P3, with the relatively unperturbed core position P1 serving as reference for each index. The reaction In^{115}(n,n') has been chosen as

denominator for the indices, partly because of the high experimental accuracy achieved for its determination and partly because its threshold of 1.2 MeV is relatively low.

The moderation effect of the central lead zone is clearly indicated by the P2/P1 ratios of the spectral indices, the value for the non-threshold reaction rate $Zn^{64}(n,\gamma)$ being greater than 1.0 and those for the higher-threshold reactions being all less than 1.0. Furthermore, the manner in which the effects of the the lead region diminish with distance is well quantified by the changes in the spectral indices between P2/P1, P3/P1, P5/P1 and P6/P1. As regards the core asymmetry created by the presence of the accelerator tube and lead zone, this is characterised by the ratios P3/P1 and P4/P1. It is seen that the differences are largely well within the indicated 1-sigma uncertainties, confirming that asymmetry effects are minor when the accelerator is not operating. The corresponding differences in the source-driven subcritical configurations are, of course, expected to be much greater.

As regards the comparison of calculational and experimental results in Table 6, agreement is seen to be well within the indicated uncertainties in most cases. The need is clearly indicated, however, for improving the statistical accuracy of some of the MCNP results.

6. CONCLUSIONS

Foil activation measurements and their interpretation have been described for the reference critical MUSE4 configuration. The different locations studied have permitted several effects to be quantified, e.g. the moderation effects of the central lead region and the relatively low degree of asymmetry of the core.

Good agreement has generally been obtained in the comparisons of the measurements with calculational results based on two different codes and data libraries. Predictions for the lead region, however, have been found to be somewhat problematic, in particular for the higher-threshold reaction rates. Differences in calculated reaction rate distributions between the JEF-2.2 and the adjusted ERALIB1 libraries (using ERANOS) have been found to be small. For the MCNP calculations, need has been indicated for improving the statistical accuracies in some cases.

The present investigations have clearly demonstrated the value of foil activation measurements in the MUSE4 programme. Use of the currently reported spectral indices for unfolding the neutron spectrum at specific locations is expected to provide useful supplementary information. Similar studies in the subcritical configurations will, of course, form the basis for the characterisation of other ADS-specific features, e.g. those related to the external source.

ACKNOWLEDGEMENTS

The MUSE4 project is being conducted at the MASURCA facility at CEA-Cadarache. We are grateful to the entire MASURCA staff for the excellent reactor operation and maintenance. Our thanks are also due to O.P. Joneja, R. Früh and J.P. Steudler for their advice and realisation of some of the experimental tools at EPFL. Finally, we acknowledge the support of the LEPh laboratory at CEA-Cadarache and would like to thank, in particular, R. Jacqmin for his collaboration.

REFERENCES

[1] R. Soule et al., "Experimental Validation of the Neutronic Characteristics of the Sub-Critical Multiplying Medium of an ADS : The MUSE Experiments", *International Conference on Accelerator Driven Transmutation Technologies and Application (ADTT'01)*, Reno, USA (2001).

[2] J.F. Briesmeister, "MCNP – A General Monte Carlo N-Particle Transport Code", *Los Alamos National Laboratory Report LA-12625*, Los Alamos, USA (1993).

[3] J.Y Doriath et al., "ERANOS1 : The Advanced European System of Codes for Reactor Physics Calculations", *International Conference on Mathematical Methods*, Karlsruhe, Germany (1993).

[4] E. Fort et al., "Realisation and Performance of the adjusted nuclear data library ERALIB-1 for calculating fast reactor neutronics", *PHYSOR'96*, Mito, Japan (1996).

[5] J. Rowlands et al., "The JEF-2.2 Nuclear Data Library", *NEA/OECD - JEFF Report 17*, Paris, France (2000).

[6] D. Villamarin et al., "Benchmark on Computer Simulation of MASURCA Critical and Subcritical Experiments (MUSE4 BENCHMARK)", *NEA/OECD - WPPT(2001)5*, Paris, France (2001).

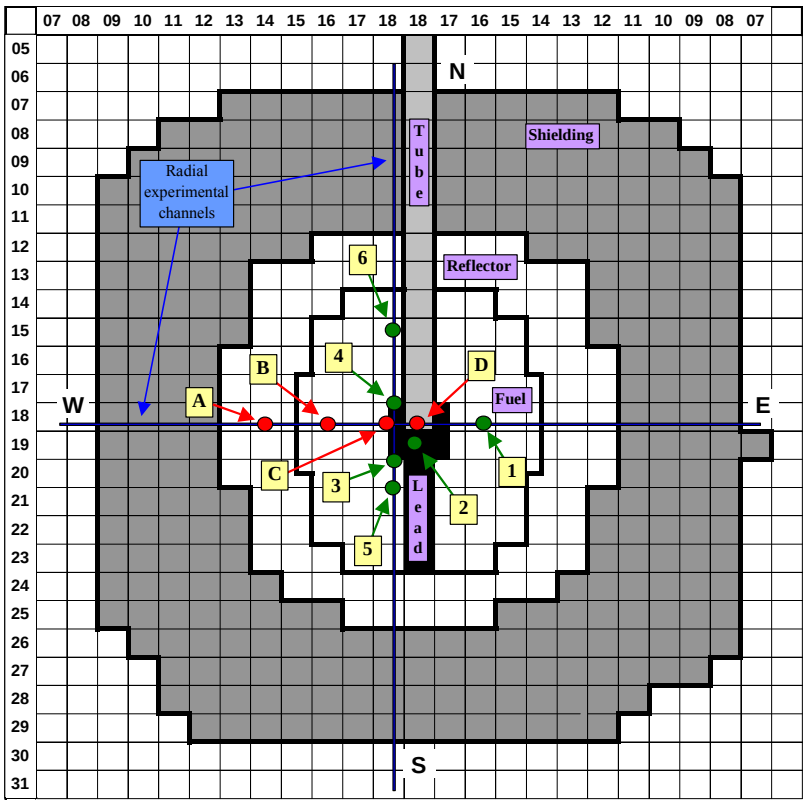

Figure 1. Horizontal cross-sectional view of the MUSE4 critical configuration, indicating the foil locations and the experimental channels (each of the square cells is 10.6cm x 10.6cm)

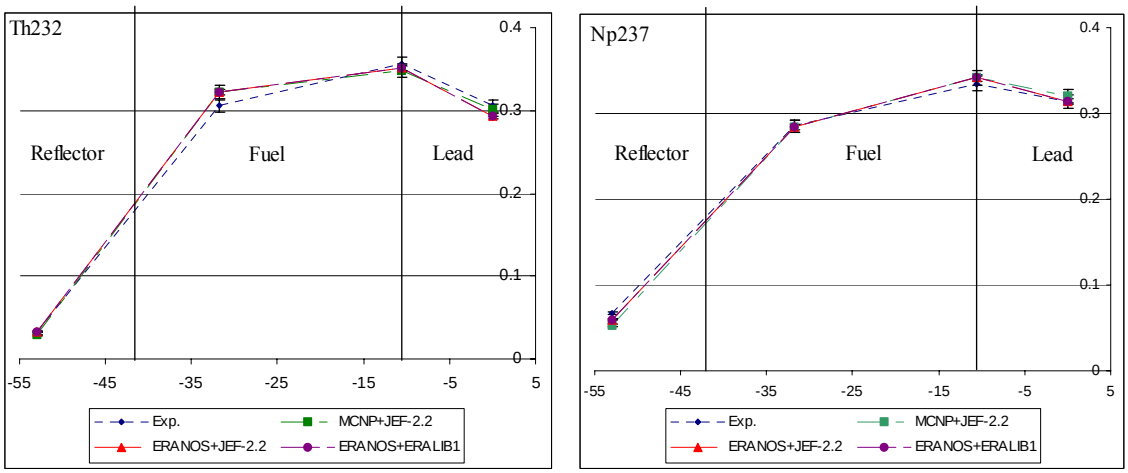

Figure 2. Np^{237} and Th^{232} fission rates along the west/east axis (The sum of the ordinates is normalised to 1.0 in each case.)

Table 1. List of the activation reactions being employed to study spectral variations in MUSE4, together with the uncertainties on measured activities

Reaction	**Threshold** [MeV]	**Uncertainty (1-sigma)** %
In115(n,γ)In116m	-	1.0
Zn64(n,γ)Zn65	-	1.5
Au197(n,γ)Au198	-	1.5
Np237(n,γ)	-	4.0
Np237(n,fis)	0.7	4.0
In115(n,n')In115m	1.2	1.0
Th232(n,fis)	1.3	4.0
Co59(n,p)Fe59	2.0	4.0
Ni58(n,p)Co58	2.8	1.0
Zn64(n,p)Cu64	2.8	3.0
Fe54(n,p)Mn54	3.1	2.0
Fe56(n,p)Mn56	6.0	2.5
Mg24(n,p)Na24	6.8	3.0
Al27(n,a)Na24	7.2	3.0
Nb93(n,2n)Nb92m	11.0	1.5

Table 2. Measured saturated activity ratios to investigate self-shielding effects

Symmetric locations On the west/east axis (in cm)	**Reaction**	**Ratio (central foil of the set / single symmetric foil)**	**Uncertainty (1-sigma) %**
(X=-47.7 / X=+47.7)	**In115(n,γ)**	0.72	4.0
(X=-37.1 / X=+37.1)	**Zn64(n,γ)**	0.85	3.0
(X=-26.5 / X=+26.5)	**In115(n,γ)**	0.97	4.0
(X=-26.5 / X=+26.5)	**In115(n,n')**	0.99	2.0
(X=-15.9 / X=+15.9)	**Zn64(n,γ)**	0.97	3.0
(X=-5.3 / X=+5.3)	**In115(n,γ)**	0.99	4.0
(X=-5.3 / X=+5.3)	**In115(n,n')**	1.02	2.0

Table 3. Calculated k_{eff} values for the MUSE4 critical configuration (experiment: 0.999)

Code/Library	**k_{eff} value**
ERANOS-1.2/ERALIB-1	1.00389
ERANOS-1.2/JEF-2.2	1.00273
MCNP-4C/JEF-2.2	1.00029
MCNP-4C/ENDF-B6	1.00836

Table 4. C/E values for the spatial variation of non-threshold reaction rates

Reaction	Code/Library	P2/P1 (C/E)	P3/P1 (C/E)	P4/P1 (C/E)	P5/P1 (C/E)	P6/P1 (C/E)
In115(n,γ)	**MCNP/JEF-2.2**	0.92 ± 0.07	0.94 ± 0.07	0.90 ± 0.07	0.94 ± 0.07	0.86 ± 0.07
	ERANOS/JEF-2.2	1.03 ± 0.02	1.02 ± 0.02	1.00 ± 0.02	1.01 ± 0.02	0.97 ± 0.02
	ERANOS/ERALIB1	1.03 ± 0.02	1.01 ± 0.02	0.99 ± 0.02	1.00 ± 0.02	1.02 ± 0.02
Zn64(n,γ)	**MCNP/JEF-2.2**	0.96 ± 0.03	1.01 ± 0.03	1.01 ± 0.03	1.01 ± 0.03	0.97 ± 0.03
	ERANOS/JEF-2.2	0.94 ± 0.02	0.96 ± 0.02	0.98 ± 0.02	0.98 ± 0.02	0.97 ± 0.02
	ERANOS/ERALIB1	0.93 ± 0.02	0.96 ± 0.02	0.98 ± 0.02	0.98 ± 0.02	0.96 ± 0.02
Au197(n,γ)	**MCNP/JEF-2.2**	0.98 ± 0.03	1.01 ± 0.03	0.96 ± 0.03	0.98 ± 0.03	1.00 ± 0.03
	ERANOS/JEF-2.2	1.04 ± 0.02	1.01 ± 0.02	0.99 ± 0.02	1.00 ± 0.02	1.02 ± 0.02
	ERANOS/ERALIB1	1.04 ± 0.02	1.01 ± 0.02	0.99 ± 0.02	1.00 ± 0.02	1.03 ± 0.02

Table 5. C/E values for the spatial variation of threshold reaction rates

Code / Library	Reaction	Threshold (MeV)	P2/P1 (C/E)	P3/P1 (C/E)	P4/P1 (C/E)	P5/P1 (C/E)	P6/P1 (C/E)
MCNP / ENDF/B6 Dosimetry File	**In115(n,n')**	**1.2**	0.89 ± 0.02	0.95 ± 0.02	1.01 ± 0.02	1.02 ± 0.02	0.96 ± 0.02
	Co59(n,p)	**2**	0.60 ± 0.06	0.84 ± 0.06	0.88 ± 0.06	1.01 ± 0.06	1.02 ± 0.06
	Ni58(n,p)	**2.8**	0.84 ± 0.03	0.94 ± 0.03	1.02 ± 0.03	1.06 ± 0.03	0.99 ± 0.03
	Zn64(n,p)	**2.8**	0.83 ± 0.05	0.96 ± 0.05	1.06 ± 0.05	1.08 ± 0.05	1.04 ± 0.05
	Fe54(n,p)	**3.1**	0.82 ± 0.04	0.93 ± 0.04	1.00 ± 0.04	1.07 ± 0.04	1.00 ± 0.04
	Fe56(n,p)	**6**	0.39 ± 0.06	0.75 ± 0.06	0.84 ± 0.06	1.00 ± 0.06	0.95 ± 0.06

Table 6. Calculated and measured spatial variations of spectral indices

Spectral index [threshold in MeV]	Type of result	P2/P1	P3/P1	P4/P1	P5/P1	P6/P1
Zn64(n,γ)/In115(n,n') [-]/[1.2]	**Experimental**	1.60 ± 0.05	1.28 ± 0.04	1.28 ± 0.04	1.14 ± 0.04	1.10 ± 0.04
	MCNP (B6 dosi.)	1.81 ± 0.09	1.40 ± 0.07	1.27 ± 0.06	1.15 ± 0.06	1.13 ± 0.06
Ni58(n,p)/In115(n,n') [2.8]/[1.2]	**Experimental**	0.70 ± 0.03	0.84 ± 0.03	0.85 ± 0.03	0.90 ± 0.04	0.95 ± 0.04
	MCNP (B6 dosi.)	0.65 ± 0.03	0.83 ± 0.04	0.85 ± 0.04	0.94 ± 0.05	0.98 ± 0.05
Zn64(n,p)/In115(n,n') [2.8]/[1.2]	**Experimental**	0.65 ± 0.04	0.81 ± 0.04	0.80 ± 0.04	0.89 ± 0.05	0.90 ± 0.05
	MCNP (B6 dosi.)	0.64 ± 0.03	0.82 ± 0.04	0.85 ± 0.04	0.95 ± 0.05	0.97 ± 0.05
Fe54(n,p)/In115(n,n') [3.1]/[1.2]	**Experimental**	0.66 ± 0.03	0.83 ± 0.03	0.86 ± 0.03	0.90 ± 0.04	0.93 ± 0.04
	MCNP (B6 dosi.)	0.64 ± 0.03	0.82 ± 0.04	0.86 ± 0.04	0.94 ± 0.05	0.98 ± 0.05